International Journal of Control and Automation
Vol. 13, No. 2s, (2020), pp. 257-267

Induction Motor Single Phasing Fault Detection using different Artificial Intelligent Techniques

[1]Rurdanarayan Dash and [1*]Sarita Samal
[1]*rudra.dashfel@kiit.ac.in,*[1*] *ssamalfel@kiit.ac.in*
[1]*School of Electrical Engineering KIIT, Deemed To be University*

Abstract
In this paper, the numbers of artificial intelligent techniques are applied to detect the induction motor single phasing fault at no load as well as different load conditions. For this work we have taken the three phase shifts between the phase voltage and line currents as the inputs to the different neural networks. The three phase shifts can be generated by conducting the number of tests of an induction motor by help of the D-Space. This paper presents a comparision between all the neural networks that how effectively it to detect the single phasing fault of a three phase induction motor. The analysis and simulated results are presented in this paper for the verification of the feasibility.
Keyword: *Artificial Intelligence Technique; Back Propagation Algorithm; Induction Motor; Single Phasing Fault;*

1. Introduction

Induction machines are very rarely used electrical motors in Industry. Though the Induction motors are very dependable, they face the different methods of failures. These failures may be inborn within the induction motor. A fault in an induction motor is an error caused by ignorance, bad judgment or intention and of decreased ability related to specify minimum requirements which results the normal wear, poor alignment, poor specification or design. If the fault is not identified or if there is any scope to grow further it may results to a failure. According to the location these faults can be of two types, that is stator faults which includes abnormal connection of the stator windings, turn to ground faults, stator core related faults and opening or shorting of the stator winding faults and rotor faults which includes rotor winding fault, bearing and gear box fault, eccentricity related fault and broken bar or cracked end ring faults as shown in the Fig. 1.

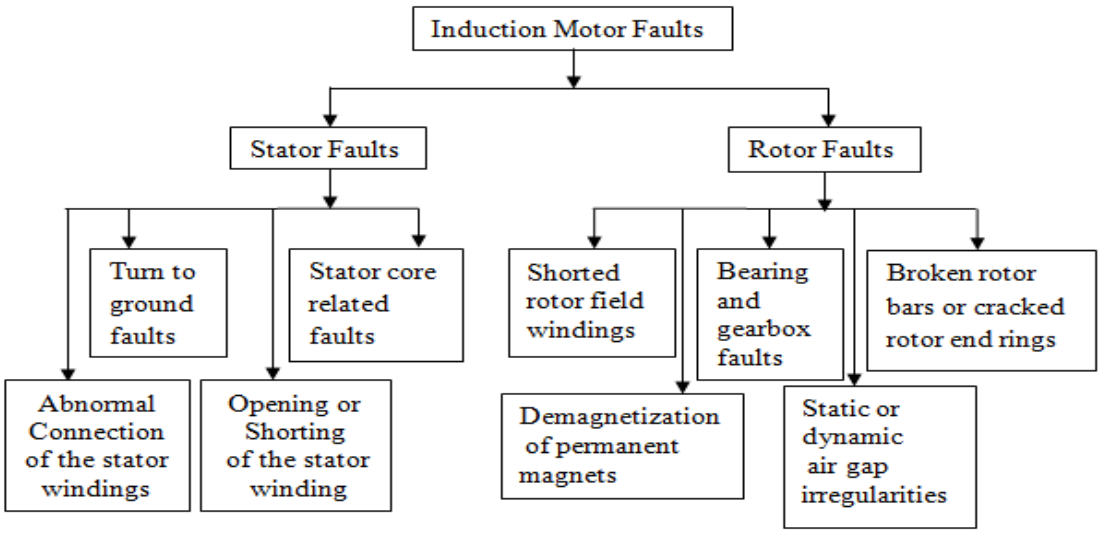

Fig 1. Sources of Induction motor faults

In an Induction motors the fault monitoring techniques are given in the literature can be classified as follows [1]-[16]. The diagnosis of a inter turn fault of a cage induction motor by using a proper model as reported in [1]. The steady state and transient behavior with short-circuited turns of

ISSN: 2005-4297 IJCA

an induction motor have been studied successfully used the models. In [2] presented the rotor broken bar and short circuit faults of a squirrel cage induction motor.

The Time frequency domain techniques which include the Bi-Spectrum, wavelet analysis and High resolution spectral analysis were used for fault detection of induction motors [3]-[7]. In paper [3] proposed the inter-turn fault and broken bar fault of an induction motor diagnosed by using the stator current. In [4] the descrete wavelet technique was used the motor current to detect the induction motor broken bar fault.

The artificial intelligence methods such as genetic algorithm, multi layer perceptron neural netwoks, adaptive neural fuzzy inference systems, support vector machines are the third methods used to detect the induction motor faults [8]-[12]. In [9] the detection of the induction motor stator winding fault by using the fuzzy logic method. In [10] the combination of the wavelet neural network and the fuzzy set theory have been used to control and identify of an uncertain system. In [13] the stator inter turn fault has been detected and located of an induction motor by using the neural network approach.The neural network techniques have the lot of advantages over the other techniques for the detection of induction motor faults [11]. These techniques give the improved performance and are very easy to modify and extend. Hence these techniques are very adaptive with the new informations and datas.

In this paper the different artificial intelligent techniques has been used to detect the single phasing fault of a three phase induction motor. The induction motor parameters at different load conditions have been generated by the help of the experiments conducted in the laboratory. The parameters are used to generate the three phase shift at no load and different load conditions. The three phase shifts has been used as the input parameters for the different artificial intelligent techniques.

2. Generation Of Motor Parameters At No Load And Different Load Conditions

The generations of the induction motor parameters at no load and different load conditions has been found by using an experimental set up. The fig. 2 shows the experimental set up for the generation of the three phase induction motor phase currents at single phasing faulty condition. For the experiment a 1 h.p, star connected three phase induction motor having the rated speed of 1435 - 1500 rpm, rated voltage of 415 Volts and rated current of 1.9 Amperes have been used.

Fig. 2. Experimental Setup to generate the induction motor parameters.

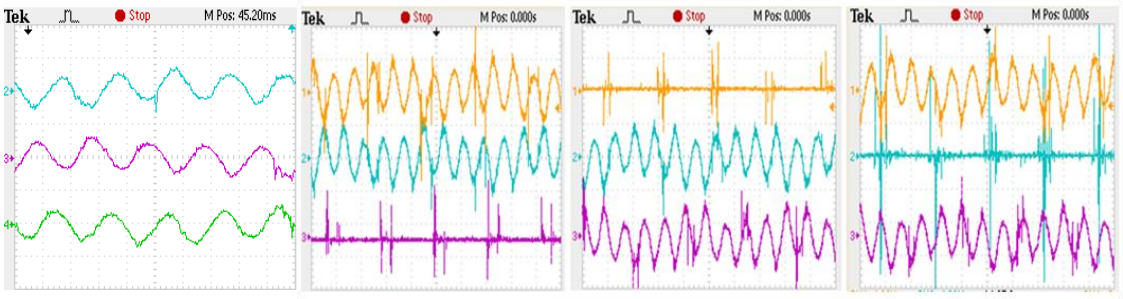

(a) (b) (c) (d)

Fig. 3 Stator currents at healthy and faulty condition at different phases at no load condition.

The fig. 3 shows the three phase currents at healthy and single phasing faulty conditions. The fig. 3(a) shows the the three phase currents at healthy condition where the magnitudes are equal and displaces by an angle of 120^0 with each other. The fig. 3(b) shows the three phase currents when a single phasing fault occurs in the R phase. The current in the R phase is drastically decreases and the currents in the other phase's increases from its rated value. fig. 3(c) shows the three phase currents when a single phasing fault occurs in the Y phase. The current in the Y phase is drastically decreases and the currents in the other phase's increases from its rated value. fig. 3(d) shows the three phase currents when a single phasing fault occurs in the B phase. The current in the B phase is drastically decreases and the currents in the other phase's increases from its rated value.

The induction motor parameters has been found as shown in the table-1, by conducting the different tests such as d.c resistance test, no load test, and short circuit test at no load, quarter load, half load and full load conditions. At healthy conditions the phase angles between the line currents and the phase voltage are equal. When a single phasing fault occurs at any phase the phase angles between the line currents and the phase voltage are unequal. The fig. 4 shows the three phase shifts at no load and the different load conditions under single phasing fault condition.

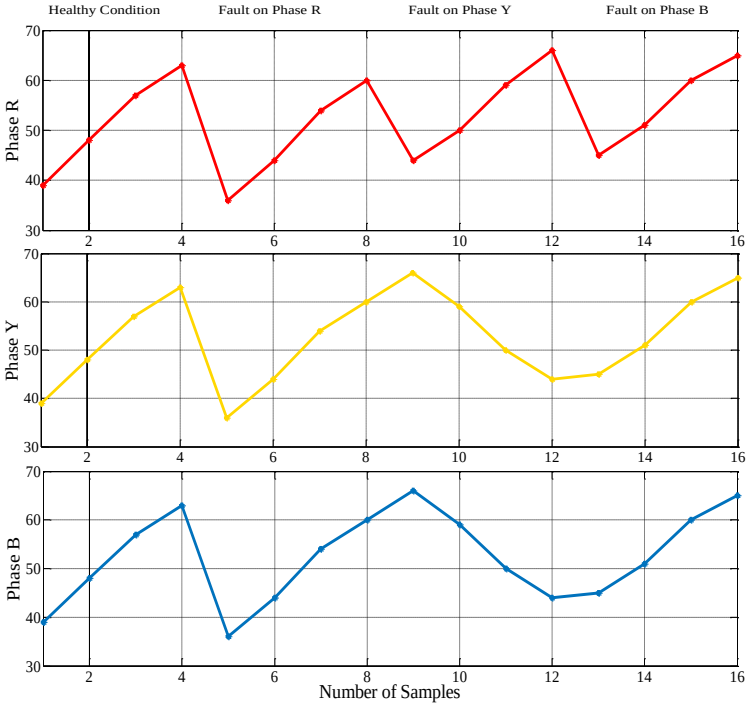

Fig. 4 Training input data set

Table I
Induction Motor Parameters under Healthy and Faulty Condition

Sl. No	Load Condition	Stator Resistance in (ohm)			Rotor Resistance in (ohm)	Stator Inductance in (Henry)			Rotor Inductance in (Henry)	Magnetizing Inductance in (Henry)		
		R_{sr}	R_{sy}	R_{sb}	R_r	L_{sr}	L_{sy}	L_{sb}	L_r	L_{mr}	L_{my}	L_{mb}
1	No load with healthy condition	9.56	9.56	9.56	8.6	0.5198	0.5198	0.5198	0.5198	0.236	0.236	0.236
2	No load with R Phase single phasing	10.56	7.68	6.96	8.6	0.072	0.1719	0.1690	0.5198	0.216	0.1123	0.10 56
3	No load with Y Phase single phasing	6.96	10.56	7.68	8.6	0.1690	0.072	0.1719	0.5198	0.1056	0.216	0.1123
4	No load with B Phase single phasing	7.68	6.96	10.56	8.6	0.1719	0.1690	0.072	0.5198	0.1123	0.10 56	0.216
5	1/4th load with Healthy condition	10.96	10.96	10.96	8.6	0.5198	0.5198	0.5198	0.5198	0.279	0.279	0.279
6	1/4th load with R phase single phasing	11.58	4.59	4.8	8.6	0.0512	0.1169	0.0916	0.5198	0.216	0.231	0.246
7	1/4th load with Y phase single phasing	4.8	11.58	4.59	8.6	0.0916	0.0512	0.1169	0.5198	0.246	0.216	0.231
8	1/4th load with B phase single phasing	4.59	4.8	11.58	8.6	0.1169	0.0916	0.0512	0.5198	0.231	0.246	0.216
9	Half load with Healthy condition	11.56	11.56	11.56	8.6	0.5198	0.5198	0.5198	0.5198	0.336	0.336	0.336
10	Half load with R phase single phasing	12.69	4.8	5.1	8.6	0.0621	0.1251	0.109	0.5198	0.284	0.296	0.291
11	Half load with Y phase single phasing	5.1	12.69	4.8	8.6	0.109	0.0621	0.1251	0.5198	0.291	0.284	0.296
12	Half load with B phase single phasing	4.8	5.1	12.69	8.6	0.1251	0.109	0.0621	0.5198	0.296	0.291	0.284
13	Full load with Healthy condition	12.74	12.74	12.74	8.6	0.5198	0.5198	0.5198	0.5198	0.436	0.436	0.436
14	Full load with R phase single phasing	13.56	5.3	5.6	8.6	0.0819	0.1497	0.137	0.5198	0.332	0.3612	0.352
15	Full load with Y phase single phasing	5.6	13.56	5.3	8.6	0.137	0.0819	0.1497	0.5198	0.352	0.332	0.3612
16	Full load with B phase single phasing	5.3	5.6	13.56	8.6	0.1497	0.137	0.0819	0.5198	0.3612	0.352	0.332

3. Fault Detection Technique

The figs. 5, 6, 7 and 8 shows the different artificial intelligent structures for the single phasing fault detection of a three phase induction motor. The three phase shifts between the line currents and the phase voltages has been used as the input to the above architechctures. The target have been given to the output layer is either 0 (when the nachine is running under healthy condition) or 1 (when a single phasing fault occurs in any phase).

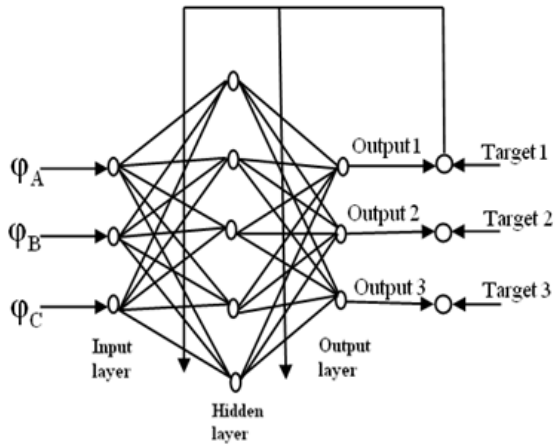

Fig. 5. MLPNN Architecture

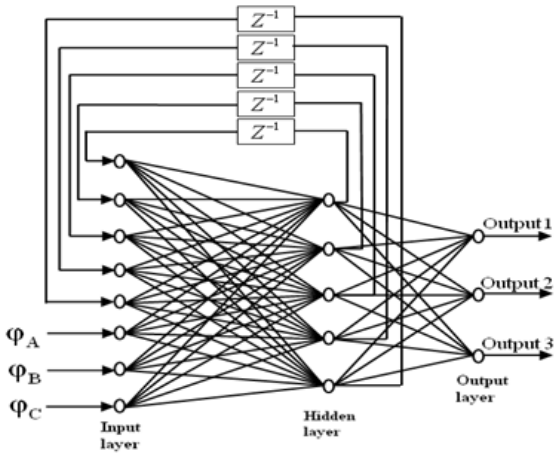

Fig.6 . RNN Architecture

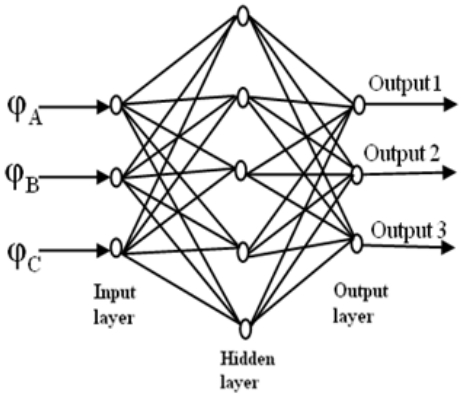

Figure 7. RBFNN Architecture

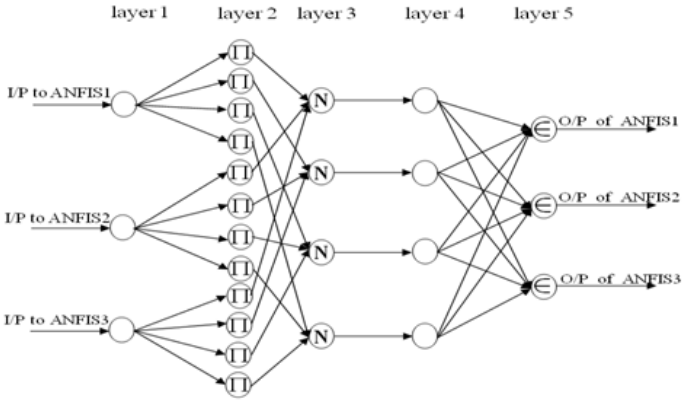

Figure 8. ANFIS Architecture

4. Results and Discussion

The figs. 9, 11 and 13 shows the output of the respective three phases where the dotted line has been taken as target value either 1 or 0, and the solid line gives the actual output by using the multilayer perceptron neural netwok. The multi layer neural networks has been achieved the target mostly. The figs. 10, 12 and 14 show the residue between the target and the actual output given in the table II.

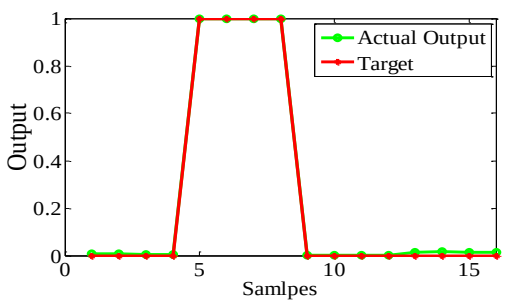

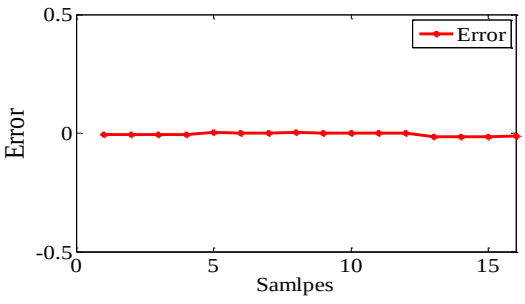

Fig.9 Output of MLPNN when fault on R phase.

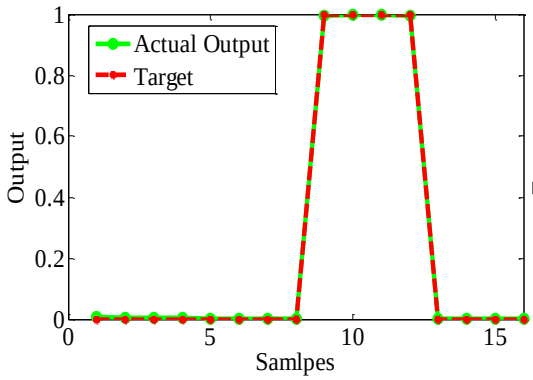

Fig.10 Error of MLPNN when fault on R phase.

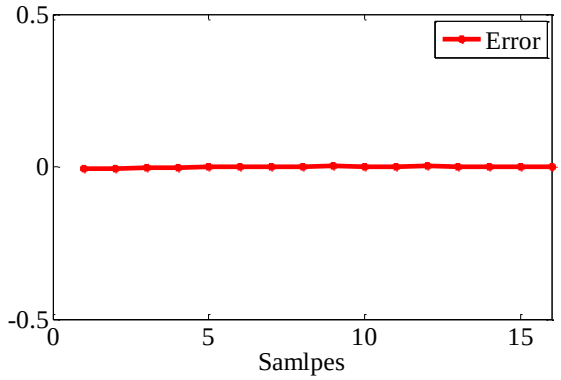

Fig.11. Output of MLPNN when fault on Y phase.

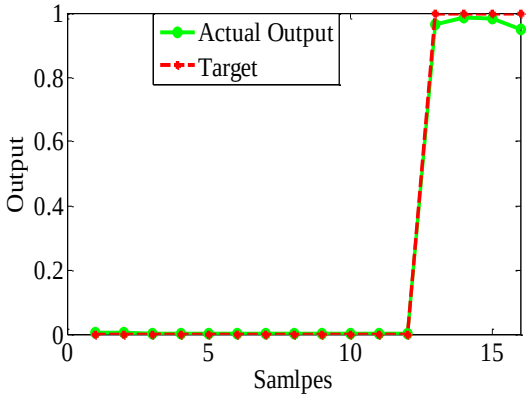

Fig.12 Error of MLPNN when fault on Y phase.

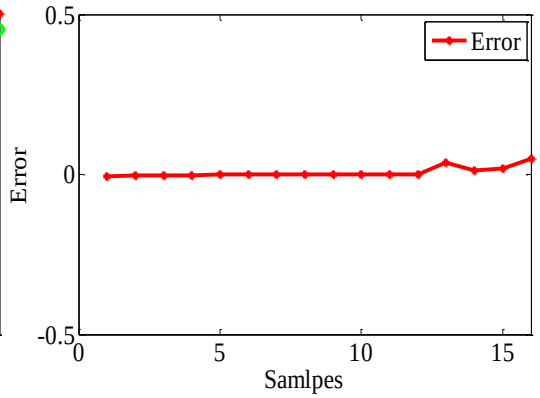

Fig.13. Output of MLPNN when fault on B phase.

Fig.14 Error of MLPNN when fault on B phase.

The figs. 15, 17 and 19 shows the output of the respective three phases where the dotted line has been taken as target value either 1 or 0, and the solid line gives the actual output by using the recurrent neural netwok. The multi layer neural networks has been achieved the target mostly. The figs. 16, 18 and 20 show the residue between the target and the actual output given in the table II.

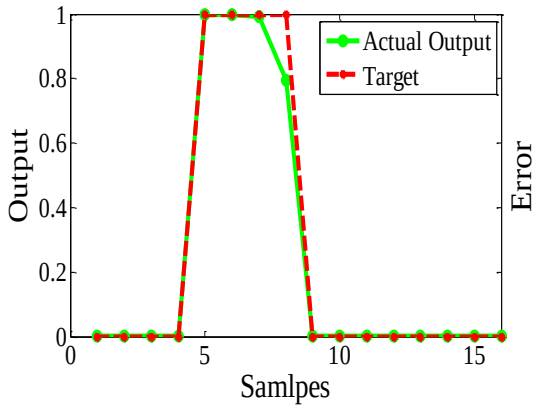

Fig.15. Output of RNN when fault on R phase.

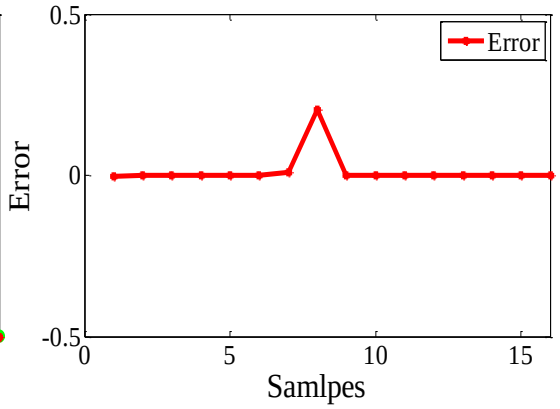

Fig.16. Error of RNN when fault on R phase.

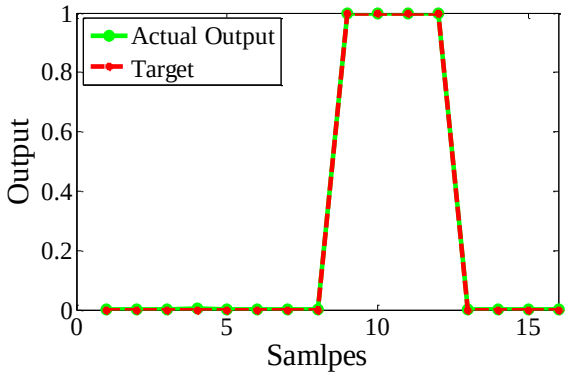

Fig.17. Output of RNN when fault on Y phase.

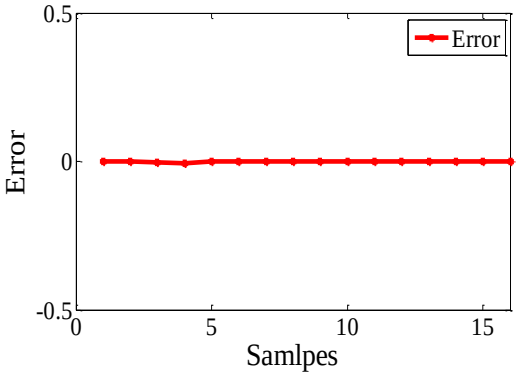

Fig.18. Error of RNN when fault on Y phase.

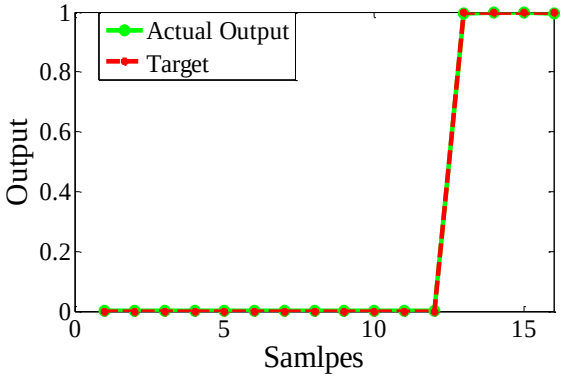

Fig.19. Output of RNN when fault on B phase.

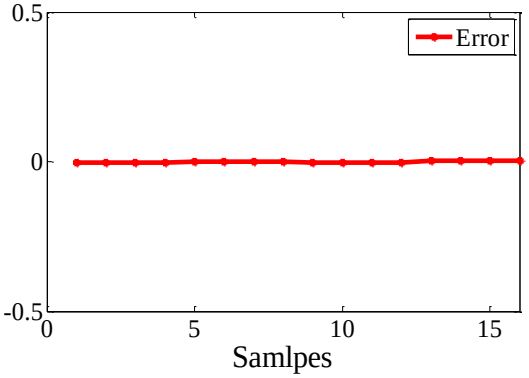

Fig.20. Error of RNN when fault on B phase.

The figs. 21, 23 and 25 shows the output of the respective three phases where the dotted line has been taken as target value either 1 or 0, and the solid line gives the actual output by using the radial basis feed forward neural netwok. The multi layer neural networks has been achieved the target mostly. The figs. 22, 24 and 26 show the residue between the target and the actual output given in the table II.

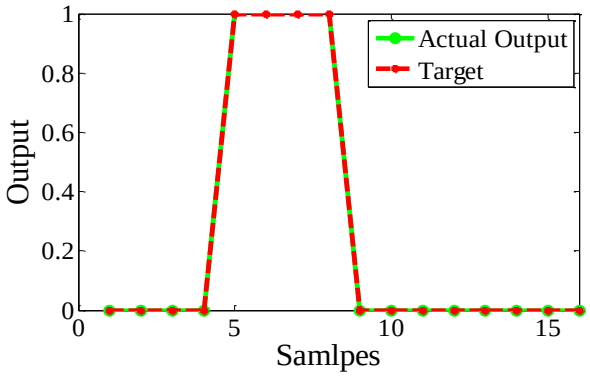

Fig.21. Output of RBFNN when fault on R phase.

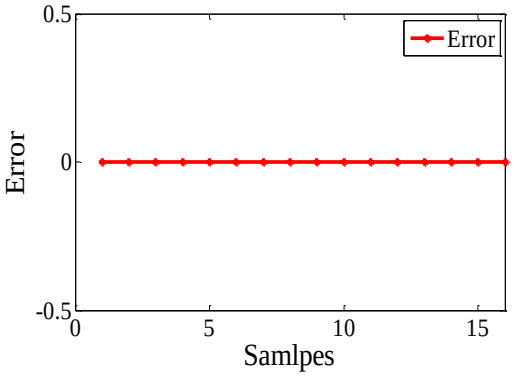

Fig.22. Error of RBFNN when fault on R phase.

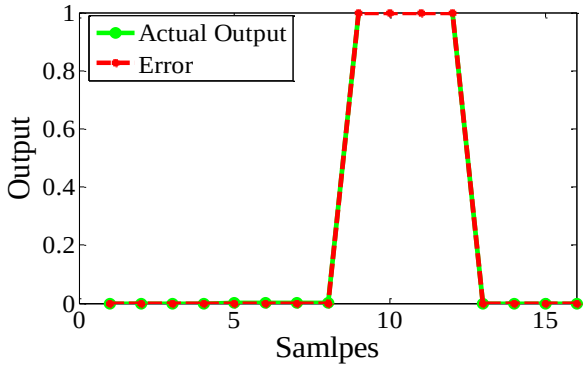

Fig.23. Output of RBFNN when fault on Y phase.

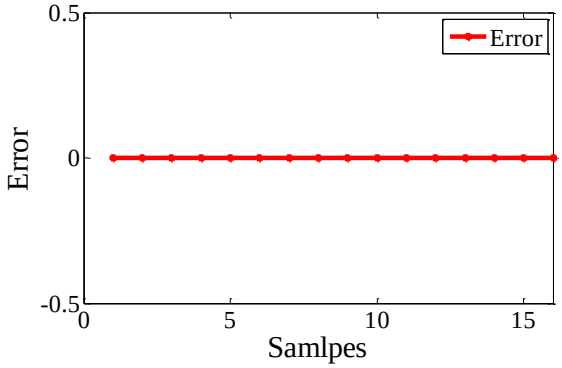

Fig.24. Error of RBFNN when fault on Y phase.

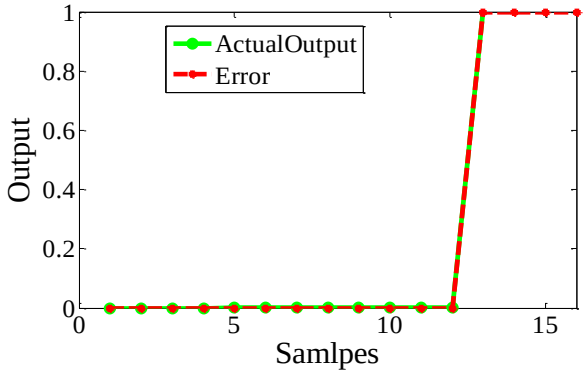

Fig.25. Output of RBFNN when fault on B phase.

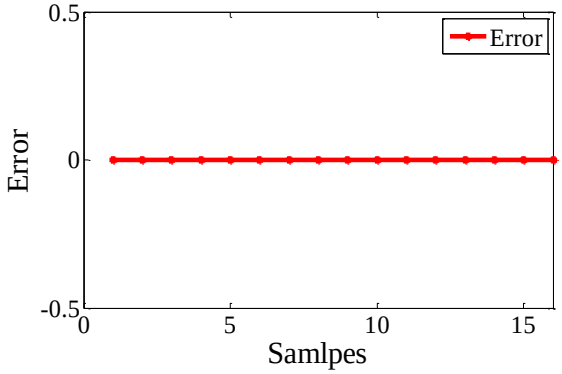

Fig.26. Error of RBFNN when fault on B phase.

The figs. 27, 29 and 31 shows the output of the respective three phases where the dotted line has been taken as target value either 1 or 0, and the solid line gives the actual output by using the ANFIS. The multi layer neural networks has been achieved the target mostly. The figs. 28, 30 and 32 show the residue between the target and the actual output given in the table II.

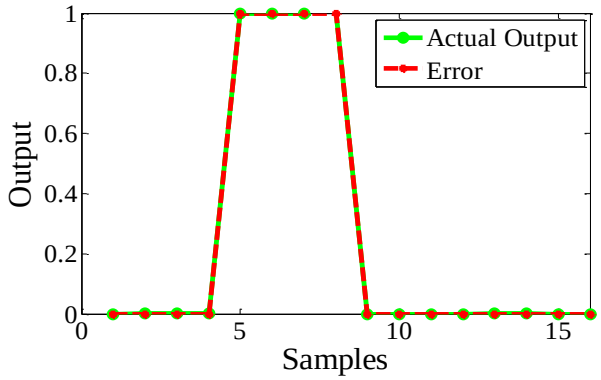

Fig.27. Output of ANFIS when fault on R phase.

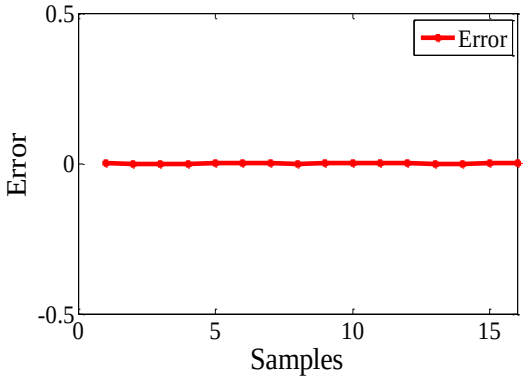

Fig.28. Error of ANFIS when fault on R phase.

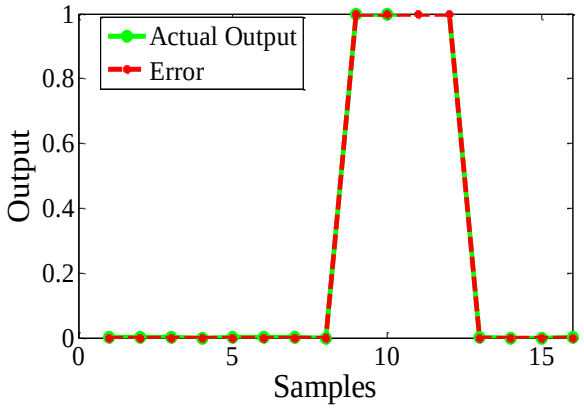

Fig.29. Output of ANFIS when fault on Y phase.

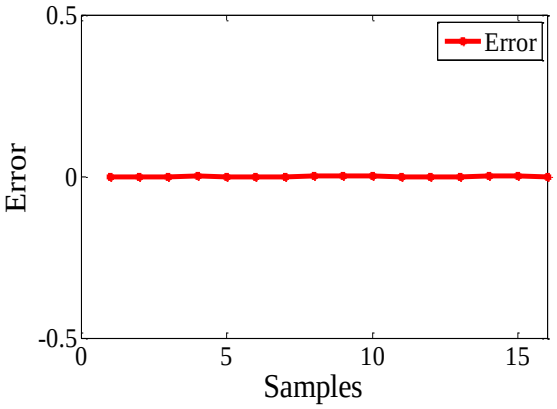

Fig.30. Error of ANFIS when fault on Y phase.

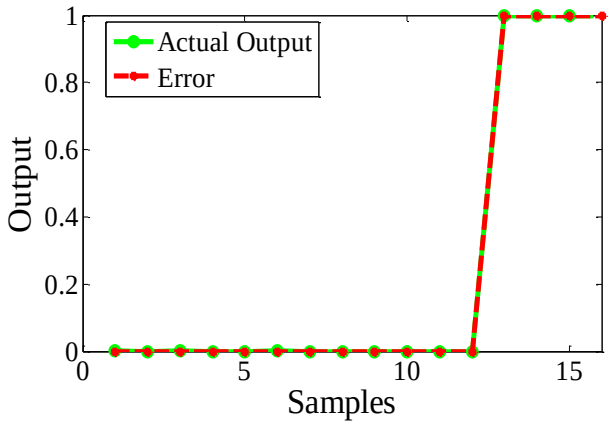

Fig.31. Output of ANFIS when fault on B phase.

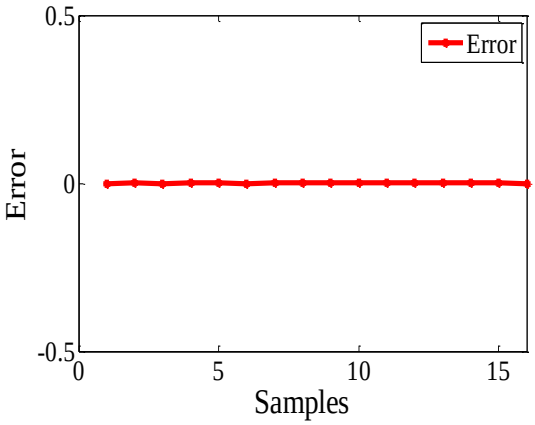

Fig.32. Error of ANFIS when fault on B phase.

The presentation of the single phasing fault diagnosis system by using different artificial intelligence technique has been judged by the mean square error (MSE) as shown in fig. 32. The training performance of the MLPNN, RNN, RBFNN and ANFIS has been compaired. The ANFIS based fault detection strategies converge quickly to wards the minimum value as comparing with other three strategies have been used. The ANFIS fault detection strategies achieves the training error as low as 8.4396×10^{-10} how ever the other strategies achieves the training errors equals to 6.9033×10^{-7}, 4.5439×10^{-5} and 7.3258×10^{-4} respectively. Hence the ANFIS based single phasing fault detection strategies presents better as compared with the other three strategy for the detection and location of the single phasing fault in the stator winding of a 3 phase induction motor. The table II gives the comparison between the training errors of each phase and the mean square error by using the different neural network paradigms.

Table II
Comparison between training errors

Training Errors	MLPNN	RNN	RBFNN	ANFIS
Fault on Phase R	6.4789×10^{-5}	0.0026	1.2326×10^{-7}	1.6098×10^{-10}
Fault on Phase Y	7.5193×10^{-6}	2.9445×10^{-6}	1.5777×10^{-7}	4.4351×10^{-11}
Fault on Phase B	2.7695×10^{-4}	5.4971×10^{-6}	2.7018×10^{-7}	3.0863×10^{-10}
MSE	4.5439×10^{-5}	7.3258×10^{-4}	6.9033×10^{-7}	8.4396×10^{-10}

ISSN: 2005-4297 IJCA

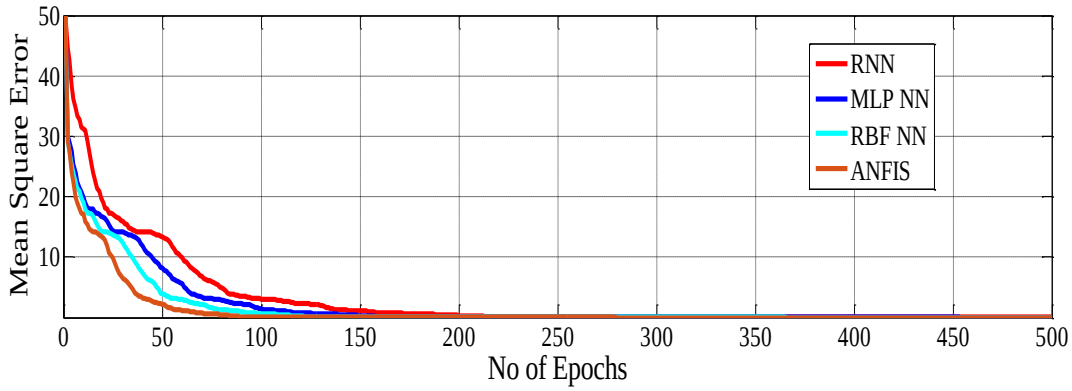

Fig.32. Comparison of the different NNs training performance.

5. Conclusion

In this paper an attempt has been made to have a methodology to diagnose the single phasing fault by opening the each phase simultaneously at different load conditions of a three phase induction motor. The data base has been obtained for the detection of the single phasing fault by conducting the series of experiments. The three phase shifts have been used as the input parameters for the neural networks paradigms. The section 4 presents the results and its analysis; it is therefore crystal clear that the single phasing fault occurring due to the open circuiting each phase has been detected. The table II gives a comparison between the training errors. Hence the accuracy of the system using ANFIS as the fault detector is more as compared with the systems using the other artificial intelligent techniques.

References:

[1] R. Isermann, "Model-based fault-detection and diagnosis—Status and applications," Annu. Rev. Control, vol. 29, no. 1, pp. 71–85, Feb. 2005.
[2] M. Arkan, D. Kostic-Perovic, P.J. Unsworth "Modelling and simulation of induction motors with inter-turn faults for diagnosis", Electric Power Systems Research, vol. 75, pp. 57-66, 2005..
[3] S. Bachir, S. Tnani, J.-C. Trigeassou, and G. Champenois, "Diagnosis by parameter estimation of stator and rotor faults occurring in induction machines," IEEE Trans. Ind. Electron., vol. 53, no. 3, pp. 963–973, Jun.2006.
[4] Aderiano M. da Silva, Richard J. Povinelli and Nabeel A. O. Demerdash, "Induction Machine Broken Bar and Stator Short-Circuit Fault Diagnostics Based on Three-Phase Stator Current Envelope," IEEE Trans. Ind. Electron., vol. 55, no. 3, pp. 1310-1318, Mar. 2008.
[5] H. Douglas, P. Pillay, and A.K Ziarani, "A New Algorithm for Transient Motor Current Signature Analysis Using Wavelets," IEEE Trans. Ind. Appl., vol. 40, no. 5, pp. 1361–1368, Sep/Oct. 2004,.
[6] M. E. H. Benbouzid et al., "Induction motors' detection and localization using stator current advanced signal processing techniques," IEEE Trans. Power Electron., vol. 14, no. 1, pp. 14–22, Jan.1999.
[7] T.W.S. Chow and S. Hai, "Induction machine fault diagnostic analysis with wavelet technique," IEEE Trans. Ind. Electron., vol. 51, no. 3, pp. 558–565, Jun. 2004.
[8] W. Thomson and M. Fenger, "Current signature analysis to detect induction motor faults," IEEE Ind. Appl. Mag., vol. 7, no. 4, pp. 26–34, Jul./Aug. 2001.
[9] Jover Rodríguez, P., Arkkio, A., "Detection of Stator Winding Fault in Induction Motor Using Fuzzy Logic," Applied Soft Computing, vol. 8, no. 2, pp. 1112-1120, 2008.
[10] Rahib Hidayat Abiyev and Okyay Kaynak, "Fuzzy Wavelet Neural Networks for Identification and Control of Dynamic Plants- A Novel Structure and a Comparative Study," IEEE Trans. Ind. Electron., vol. 55, no. 8, pp. 3133–3140, Aug. 2008,.

[11] F.Filippetti, G.Franceschini, and C.Tassoni, "A Survay of AI Techniques Approach for induction machines on-line Diagnostics," in Proc.PEMC'96, vol.2, pp. 314–318, 1996.
[12] M. Awadallah and M. Morcos, "Application of AI tools in fault diagnosis of electrical machines and drives—An overview," IEEE Trans. Energy Convers., vol. 18, no. 2, pp. 245–251, Jun. 2003.
[13] M. Ben Khader Bouzid, Gérard Champenois, Najiba Mrabet Bellaaj, Laurent Signac, and Khaled Jelassi, "An Effective Neural Approach for the Automatic Location of Stator Interturn Faults in Induction Motor" IEEE Trans. Ind. Electron., vol. 55, no. 12, pp. 4277-4289, Dec. 2008.
[14] H. Douglas, P. Pillay, and A. Ziarani, "Broken rotor bar detection in induction machines with transient operating speeds," IEEE Trans. Energy Convers.,vol.20, no. 1, pp.135-141, Mar. 2005.
[15] A. R. Mohanty and C. Kar, "Fault detection in a multistage gearbox by demodulation of motor current waveform," IEEE Trans. Ind. Electron. vol. 53, no. 4, pp. 1285–1297, Aug. 2006.
[16] F. Briz, M. W. Degnert, P. Garcia, and D. Bragado, "Broken rotor bar detection in line-fed induction machines using complex wavelet analysis of startup transients," IEEE Trans. Ind. Appl. , vol. 44, no. 3, pp. 760–768, May/Jun. 2008.
[17] S. Rajagopalan, J. M. Aller, J. A. Restrepo, T. G. Habetler, and R. G. Harley, "Analytic-wavelet-ridge-based detection of dynamic eccentricity in brushless direct current (BLDC) motors functioning under dynamic operating conditions," IEEE Trans. Ind. Electron. , vol. 54, no. 3, pp. 1410–1419, Jun. 2007.
[18] Z. Ye, B. Wu, and A. Sadeghian, "Current signature analysis of induction motor mechanical faults by wavelet packet decomposition," IEEE Trans. Ind. Electron. , vol. 50, no. 6, pp. 1217–1228, Dec. 2003.
[19] J. Cusido, L. Romeral, J. A. Ortega, J. A. Rosero, and A. Garcia Espinosa, "Fault detection in induction machines using power spectral density in wavelet decomposition," IEEE Trans. Ind. Electron. , vol. 55, no. 2, pp. 633–643, Feb. 2008.
[20] J. Antonino-Daviu, M.Riera-Guasp, J. Roger-Folch, and M. P. Molina," Validation of a new method for the diagnosis of rotor bar failures via wavelet transformation in industrial induction machines," IEEE Trans. Ind. Appl., vol. 33, no. 4, pp. 990–996, Jul./Aug. 2006.
[21] C. S. Burrus, R. A. Gopinath, and H. Guo, Introduction to Wavelets and Wavelet Transforms. A Primer. Englewood Cliffs, NJ: Prentice- Hall, 1998.
[22] R.Dash, B.Subudhi, S.Das and A.Mishra, "Neural network and wavelet techniques for detection of interturn short circuit fault in stator winding of an induction motor," international journal on power system optimization and control, vol.1, no. 2, pp. 57-63, jul-dec. 2009.
[23] M. Riera-Guasp, J. Antonino-Daviu, J. Roger-Folch, and M. P. Molina, "The use of the wavelet approximation signal as a tool for the diagnosis and quantification of rotor bar failures," IEEE Trans. Ind. Appl., vol. 44, no. 3, pp. 716–726, May./Jun. 2008.
[24] M. Riera-Guasp, Jose A. Antonino-Daviu, M. Pineda-Sanchez, R. Puche-Panadero, J. Perez-Cruz, "A general approach for the transient detection of slip-dependent fault components based on the discrete wavelet transform," IEEE Trans. Ind. Electron. , vol. 55, no. 12, pp. 4167-4180, Dec. 2008.

ISSN: 2005-4297 IJCA